Egyptian Journal of Geology

https://egjg.journals.ekb.eg

Depositional Environment and the Trapping Mechanism for the Gas and Condensate in the Messinian Level III sequence Abu Madi Formation, Nile Delta, Egypt

Ahmed Mohamed

Department of Geology, Faculty of Science, Mansoura University, El-Mansoura, Egypt

The Abu Madi Level III Messinian sequence is interpreted to have been deposited as valley-fill sediments within a pre-existing paleo-valley during a regressive-transgressive sedimentary cycle. The valley was most likely created during the Messinian salinity crisis, which happened because of the closure of the marine passages between the Atlantic and Mediterranean. Core photos, FMI images, well logs and composite logs were used to identify the depositional environment and petroleum system in the study area. From the cored photos and image logs, the river system feeding sand into the Mediterranean was a sand-dominated braided river. The channels making up the braided system were on average 150 feet wide. Following the regression, the valley was flooded, and the over-bank deposits took over. Reservoirs in the fluvial section are very clean and well-sorted. Their shape is elongated, parallel to the paleo-flow and most likely interconnected over the entire width of the fluvial tract. Reservoirs in the over-bank section have a higher shale content compared to the fluvial system. The shape of these reservoirs is most likely restricted sheet-like parallel to the valley system confining boundaries. Condensate is stratigraphically trapped in the fluvial section, which is pinching out into floodplain deposits. Gas is mainly structurally trapped in the floodplain and fluvial reservoirs.

Keywords: Abu Madi; Level III; Messinian; braided river, Nile Delta, Egypt.

1. Introduction

The Nile Delta represents a consequence of the interplay between the Nile River and the Mediterranean Sea systems. The understanding of this complex provides the clue that unlocks the possibilities and vision of significant petroleum reserves (Metwalli 2000). The Nile Delta Basin is considered the most prolific province for gas production in Egypt. The Lower Oligocene to Pliocene sequence hosts the main gas reservoirs in the Nile Delta (Nabawy et al. 2018). It was first formed during the Late Eocene, after the Nile drainage system began near the Qattara Depression in the Western Desert of Egypt (Said 1990; Sestini 1995). The delta later shifted to its current location during the Late Miocene, after a major change in the Nile's course during the Messinian salinity crisis (MSC) (Issawi and McCauley 1992; Fielding et al. 2018; Leila et al. 2018; Claudio et al. 2019). The gradual desiccation of the Mediterranean, caused by the reduced inflow of Atlantic Ocean water, led to salt deposition in deep basins and widespread erosion on the Mediterranean margins (Hsü et al. 1973; Barber 1981; Clauzon 1982; Willett et al. 2006; Bache et al. 2009; Leila and Moscariello 2019). The Nile Delta appears to be more strongly developed on its eastern flank, due to longshore currents sweeping large amounts of fluvial deposits eastward. However, the ancient distributaries largely disappeared due to dam construction and intensive irrigation in the onshore delta plain.Currently, they were eventually reduced to the western Rosetta and the eastern Damietta.

This study targeted the El Mansoura concession, which is located on the eastern flank of the Nile Delta (**Fig. 1**). It lies within one of many deeply incised valleys around the Mediterranean, which formed during the Messinian salinity crisis.

*Corresponding author e-mail: agomaa@mans.edu.eg
Received: 27/03/2023; Accepted: 10/04/2023
DOI: 10.21608/EGJG.2023.202587.1042

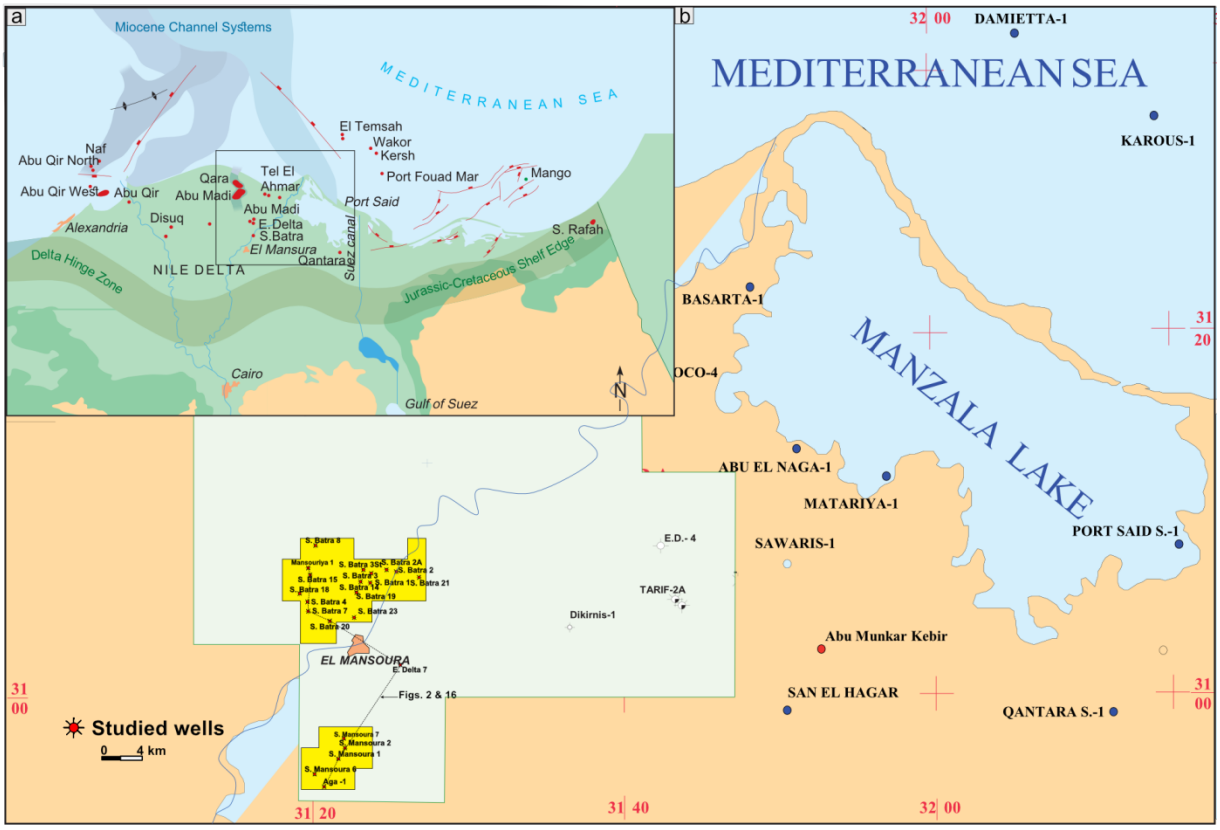

Fig. 1. a) The major tectonic events and structural patterns influencing the Nile Delta (afterSchlumberger, 1995); b) Location map of the study area (Modified from Merlose, 2007).

This erosional unconformity is clearly traceable on the seismic lines. The incised valley is recognized as the Abu Madi valley, which can be traced on seismic for over 150 km. It deepens northward till 3.5 km and is about 16 km wide in the El Mansoura area. The filling of this valley contributes to the formation of the major reservoir of the play (Duggen et al. 2003).

The current study investigated the Upper Miocene Abu Madi Formation (**Fig.2**), which is composed of a series of transgressive cycles. The Abu Madi Formation was divided into three levels (III, II, and I; **Fig.2**) based on the backstepping infill succession and the subsequent vertical transition from fluvial to estuarine and marine facies (El Adl, et al. 2021). This work focuses mainly on the fluvial section within the Level III sequence to get a better understanding of the type of river system that created the most prominent sediment package and its influence on younger sedimentation patterns. The ultimate aim of this study is to perform a comprehensive study of the geology of the Abu Madi Level III interval in the El Mansoura field in order to improve our ideas about the environment of deposition in this area and to determine the relevant changes and variations within these environments.Furthermore, the study also aims to offer a better understanding of the petroleum geological aspects in this developing field, including reservoir development, shape and potential size, hydrocarbon expulsion and trapping considerations, and provide a sedimentological framework from which seismic interpretation will undoubtfully improve exploration efficiency.

2. Materials and Methods

Sedimentological analysis of the cored intervals from the South Mansoura-1, South Batra-4, and South Batra-14 wells was carried out at a vertical scale of 1:50. For the purpose of study, a detailed sedimentological analysis comprised identification and characterization of lithologies, sedimentary structures, lithofacies types, and groups, was run. Interpreting the depositional environment followed the standard literature (e.g., Cant 1988; Reineck and Singh 1980). In addition, the Formation Micro-Imager (FMI) tool is employed for 9 wells. Detecting the sedimentary structures using the FMI was carried out on the Geoframe platform (Lloyd et al. 1986 and Serra 1989). The procedural workflow adopted for the study involves the first phase of basic processing of

the image data to generate equalized and normalized images, and then the processed images for interactive dip computation using BorView module.

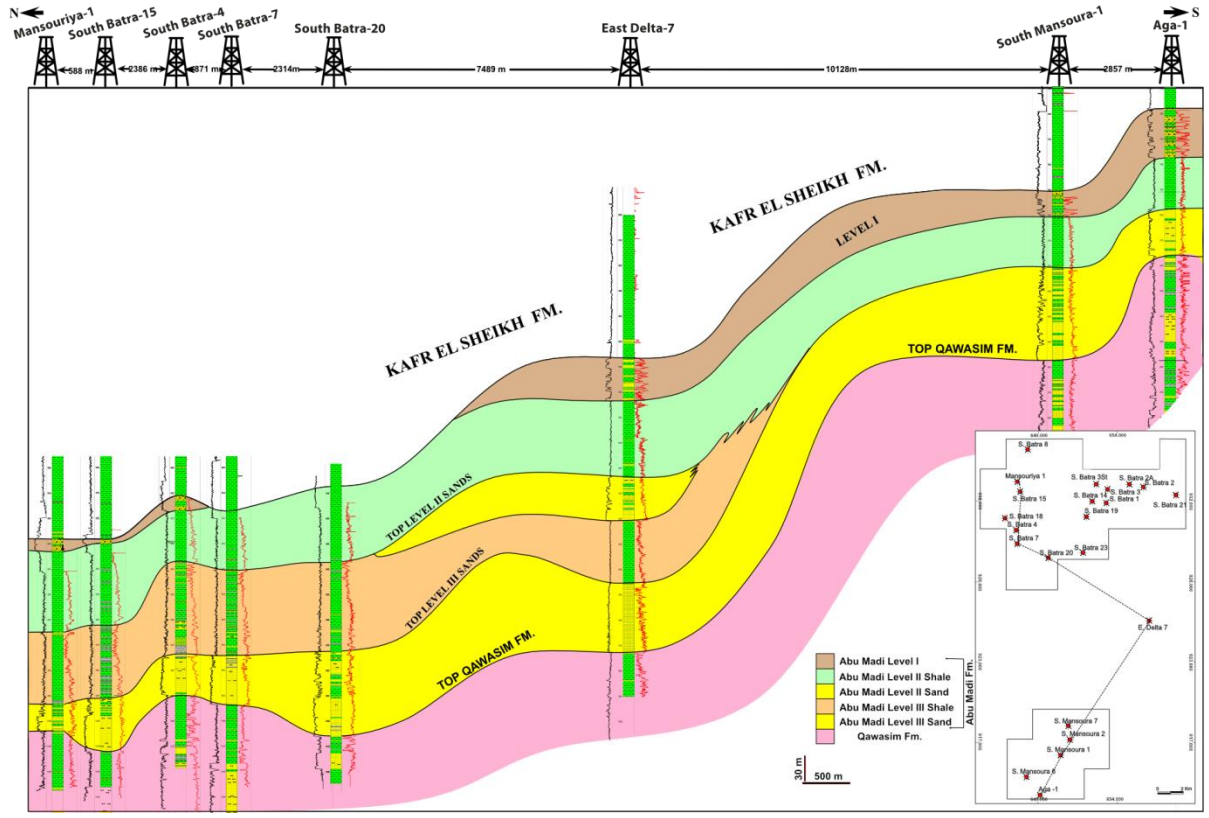

Fig. 2. North-South geological cross-section through the Upper MioceneAbu Madi Formation.

3. Results

3.1 Lithofacies

Five facies have been identified within the Abu Madi Level III sequence based on the core's observable physical and biological characteristics. These features include sedimentary structures, lithologic composition, and grain size.

3.1.1 Conglomeratic sandstone facies (F1)

This lithofacies is greenish gray, light gray, moderately indurated, and consists of vertical stacked conglomeratic sandstone displaying a fining-up vertical trend. It contains common pebble to cobble grade lithic clasts in a coarse-grained kaolinitic sand matrix. Subrounded to rounded-elliptical lithic clasts include dark gray, gray-greenishclaystones, chert, quartz, and carbonates (**Fig.3a, b**). The coarse-grained size of this lithofacies represents channel-fill deposits. Also, the absence of sedimentary structures could indicate rapid sedimentation (Miall 1977; Galloway and Hobday 1983).

3.1.2 Crossbedded sandstone facies (F2)

This lithofacies is light gray, greenish- gray, moderately to well cemented, locally highly calcareous cemented, and medium to coarse-grained. It is moderately to poorly sorted, cross-bedded, and contains common carbonaceous debris concentrating along the bedding plane (**Fig.3c**). It generally displays vertically stacked fining-up vertical trend with coarser (conglomeratic sand facies) at the base grading-up to relatively finer and cross-bedded sand. The cross-bedded sandstone lithofacies implies a fluvial channel depositional setting (Leeder 1973, Miall 1977). The complete absence of bioturbation and tidal as well as wave-structures also reflects fresh-water conditions (Miall 1977).

3.1.3 Structureless massive sandstone facies (F3)

This lithofacies is light greenish gray, patchy calcareous cemented, medium to coarse-grained moderately sorted, massive appearance, and rare argillaceous laminae (**Fig.3d**). This facies lacks any bioturbation and sedimentary structures. The massive sand bodies are interpreted as channel-fill deposits of braided rivers. Moreover, the absence of stratification indicates rapid sedimentation where there was insufficient time for bedforms to develop.

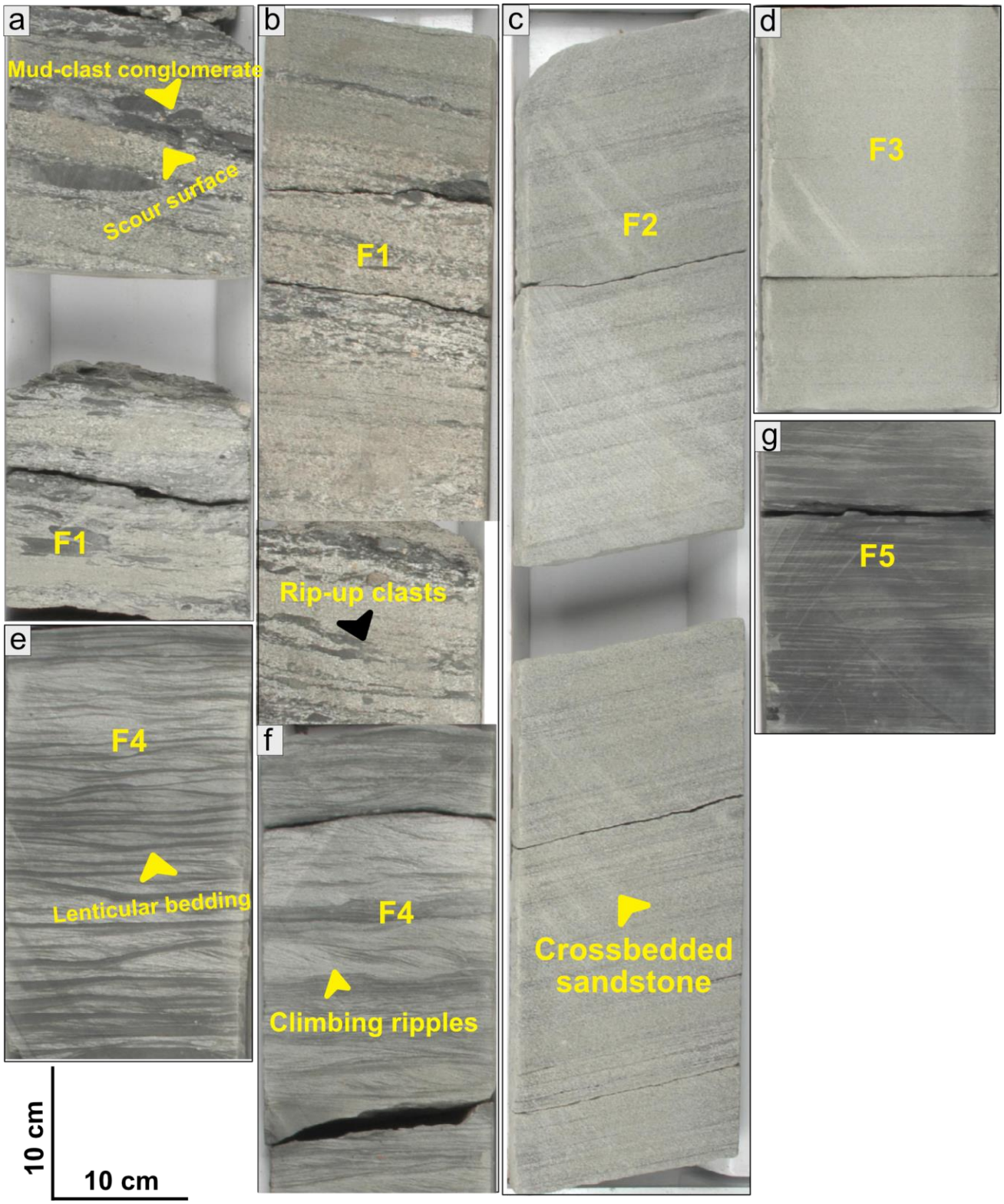

Fig. 3. Core photos showing a, b) Conglomeratic sandstone facies (F1); c) Crossbedded sandstone facies (F2); d) Structureless massive sandstone facies (F3); e, f) Flaser or lenticular bedded sandstone and mudstone facies (F4) and g) Mudstone/Siltstone facies (F5).

Galloway and Hobday (1983) suggested that this lithofacies wasa channel-fill deposit, which occupies interbar areas and accumulated as lenses of bed load sediment which can be preserved in aggrading channels. The massive coarse-grainedsandstones represent high-energy depositional facies similar

tothose accumulated at the river mouths (Reineck and Singh 1980; Orton and Reading 1993). The complete absence of mudstone further supports this interpretation interbeds or mud drapes suggesting continuous episodes of increased hydrodynamic energy (Miall 1977).

3.1.4 Flaser or lenticular bedded sandstone and mudstone facies (F4)

This lithofacies is light greenish gray, light grayand slightly to moderately calcareous cemented.It is moderately to well indurated, variably calcareous cemented, fine to medium grained, ripple to cross laminated with common argillaceous and carbonaceous laminae between ripple/cross-bed sets, finer with common wavy argillaceous and lenticular ripple lamination towards the base, displaying an overall coarsening-up vertical trend (**Fig.3e**).The presence of cross-laminated sandstone with the absence of bioturbation points to fluvial channel depositional environment (Miall 1977).The presence of horizontal stratification within the fine-grained sequence indicates that this lithofacies was deposited as inter-channel bar (Galloway and Hobday 1983). In addition, deposition of very fine sediments along the laminae and bedding planes indicates low-energy depositional conditions.

3.1.5 Mudstone/Siltstone facies (F5)

This lithofacies is composed of dark gray colored mudstone intervals generally centimeters-thick, which are restricted to the upper part of the Abu Madi Level III (**Fig.3f**). The mudstones of these facies are partly laminated, silty, and/or deformed and are typically interlaminated/interbedded with relatively rippled fine-grained sandstone units. The abundance of fine-grained sediments in this lithofacies suggests deposition in an abandoned channel bar. The presence of a thin mudstone bed at the top of the fining-upward sequence is consistent with the upward reduction of the hydrodynamic energy and most likely represents the fluvial floodplain or over-bank deposits (Miall 1977; Leila and Moscariello 2019).

3.2 Facies associations and depositional environment

Within the cored successions, three facies associations can be distinguished (**Fig.4**): (i) Fluvial channel-fill environment, which constitutes the lower part of the Abu Madi level III and consists of conglomeratic sandstone facies (F1), (ii) Vertically stacked fluvial channel bars which occur above the fluvial channel-fill deposits and consist of crossbedded sandstone facies (F2) and structureless massive sandstone facies (F3), and (iii) Over-bank deposits, which dominate the upper part of the Abu Madi level III and consist of the flaser or lenticular bedded sandstone and mudstone facies (F4) and mudstone/Siltstone facies (F5).

3.3 FMI Image Log Data

The image log (FMI) data from both cored and non-cored intervals were used to evaluate lithofacies, depositional elements, and paleo-current direction (Tucker 2001; Donselaar and Schmidt 2005; Folkestad et al. 2012; Miall 2014; Lai et al. 2018; Hassan et al. 2022). The FMI data offered a more detailed examination of the lithofacies, as well as a better understanding of the depositional environment and associated sedimentary structures. Based on the seismic and amplitude maps, the studied area is divided into three channels. **Figure 5A** is an amplitude map on the Abu Madi Level III horizon, which shows higher amplitudes, indicated by warmer colors, on the western and eastern side of the valley separated by an area with cooler colors. It is suggested that these warmer colors are indications of the presence of sand. The Abu Madi Level III, spectral decomposition map also supports this evidence (**Fig. 5B**).

3.3.1Western channel FMI analysis

The sequence has a general fining upward trend, becomes thinner to the top and has a sharp, erosive base (**Fig.6**). Two coarser streaks of conglomerate are observed near the base of the sequence. This zone is characterized by medium to high-angle cross-bedding with a NW to NE trending. The dominant direction is to the NNE (**Fig.6**). Towards the top of the sandstone package, the sands become thinner, bedded and display a lenticular nature. In this upper sequence, crossbed orientations are more variable than at the base of the sequence, but NW-NE crossbeds still predominate (**Fig.6**).

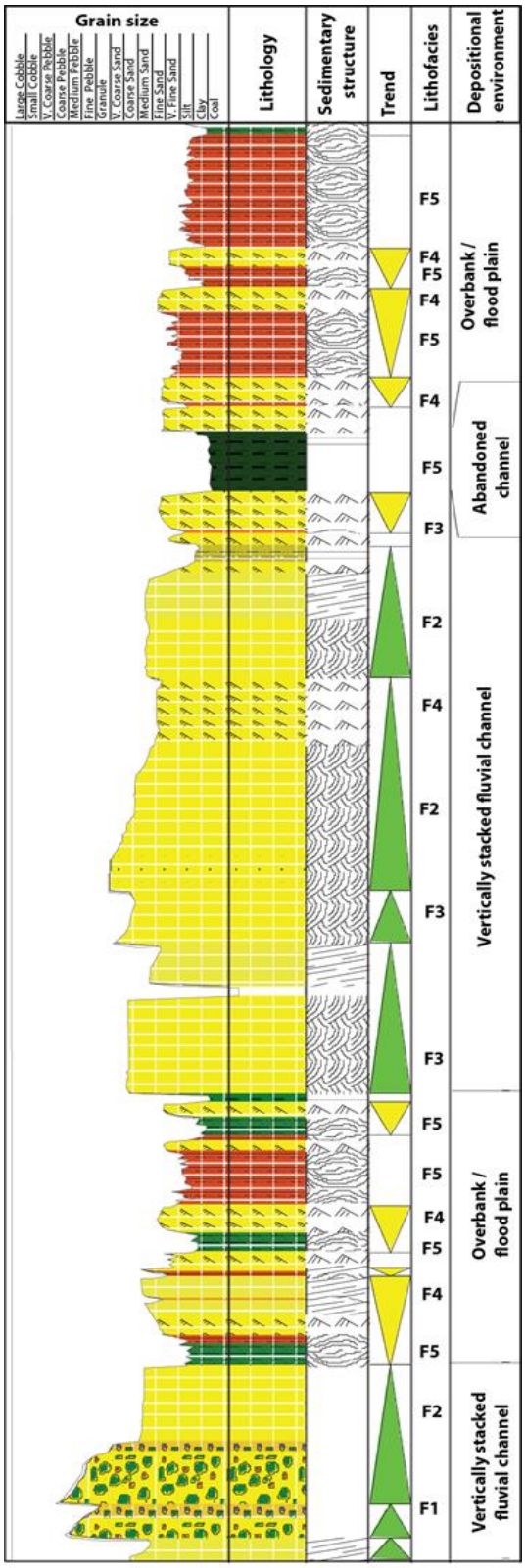

Fig. 4. Lithofacies log showing the different lithofacies and suggested depositional environment for each association.

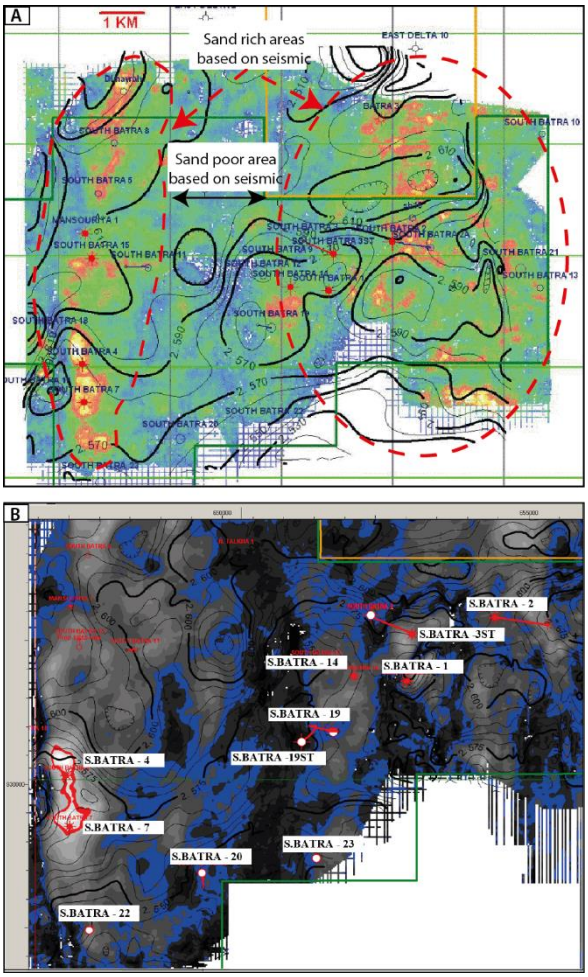

Fig. 5. A) Isochron of the Abu Madi Level III combined with amplitude map. Warm colors indicate high amplitudes believed to be associated with the presence of sand. Black contours are time contours with a 10ms contour interval corresponding to roughly 45 feet. B) The spectral decomposition map at Abu Madi Level III.

Bed thickness ranges from 1ft to 8 ft in the sandy part, with an average bed thickness of 3.5 ft (**Fig.6**). Beds are separated by either highly resistive streaks, which are presumed to be cemented layers, or by a change in crossbed orientations. In the middle part of the sand package, there is a 20’ thick zone where the bedding becomes fainter and there is a wider range of crossbed orientations (**Fig.6**). The top of the sequence consists mainly of parallel mudstones beds with thin interbedded tabular sandstones. Ripple marks and soft sediment deformation can be detected.

To sum up, the sequence represents an overall transgressive system starting with a low-sinuosity, fluvial system such as a braided river system at the base. This could be interpreted, based on the relatively sharp base and the abundant crossbeds with a narrow range of crossbed orientations in the sandstone. A

conglomerate interval resulting from channel bank collapse containing irregular bedding and large deformed shale clasts with chert and other rock fragments overlies this section. As the system gradually deepens near the middle of the sequence, finer-grained materials become more dominant. These deposits were thought to be deposited in an over-bank environment.

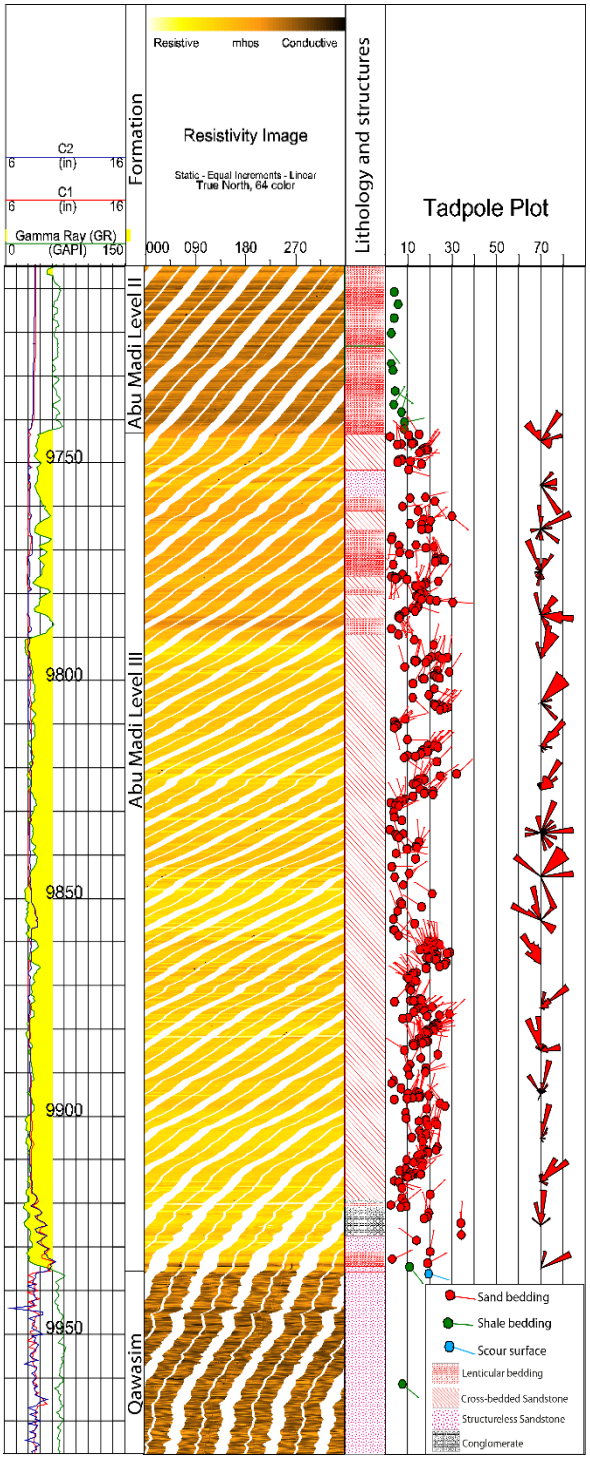

Fig. 6. FMI of the Level III sequence (South Batra-7 well).

3.3.2 Eastern channel FMI analysis

This sequence displays a fining upward trend (**Fig.7**), bed thickness becomes thinner to the top of the sequence and ranges from tens of feet near the base to inches at the top of this package. In places, internal structures are extremely faint, where bedding is homogenous. Parallel bedding to low-angle crossbedding can be observed in numerous zones with a northeastern azimuth (**Fig.7**).

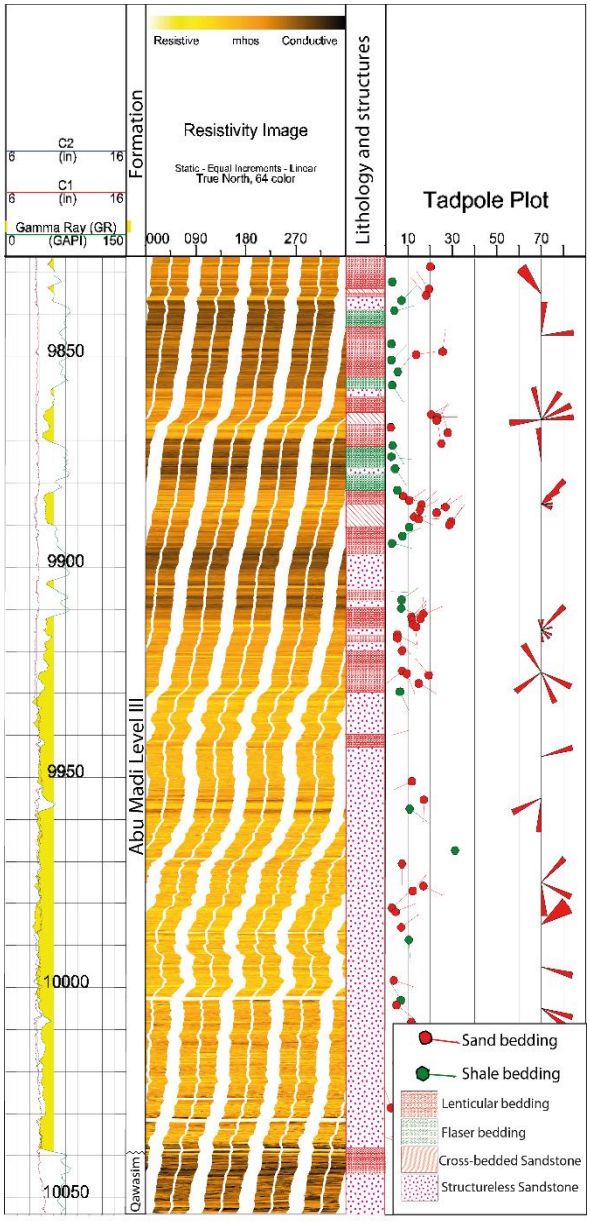

Fig.7. FMI of the Level III sequence (South Batra-2 well).

Although the overall sequence is getting finer to the top, individual beds do not indicate a similar trend. Typically, individual beds do not show much grain size variation, except to define bedding surfaces in

laminated or crossbedded sections.The finer-grained interval near the top of the sequence shows a piece of evidence of severe deformation. The bedding is tilted at high angles and appears deformed in discreet sections. The consistent east orientation of this deformed section suggests a deepening of the section in that direction.

The sequence is interpreted to result from a minor transgression within a pre-existing valley system. The lowermost sandstone is interpreted to be a result of a floodplain environment deposited in a possible laterally restricted valley.

3.3.3Central channel FMI analysis

The sequence shows a generally fining-up trend with several coarse conglomeratic streaks (**Fig.8**). The sands are well sorted near the base and characterized by medium to high-angle crossbedding with a dominant orientation to the NE, whereas minor variations in orientation were observed (**Fig. 8**). The individual beds are from 0.5 ft to 10 ftthick and typically show a fining-up texture. Interbedded with these sandstones are numerous sections containing thin-bedded sand and shale sequences that in the core are seen to contain ripple bedding (**Fig.3f**) and small-scale, low to high-angle crossbedding (**Fig. 8**). Fine-grained intervals containing thin irregular sandstone beds occur in assembly within these beds. This lower interval grades into finer-grained sediments containing mostly parallel bedding. Sands in the upper part of the sequence typically contain low to medium crossbeds with a wide variety of orientations (**Fig. 8**). Lenticular and flaser bedding become dominant upward (**Fig. 8**). At the top of the sequence, well-bedded silts and shales dominate (**Fig. 8**). Bedding is typically parallel with only minor deformation structures. In several intervals, the interbedded sands become slightly more abundant and may reach 1ft thick. These sands show vague fining-up textures as well as a thinning of bed thickness.

The sequence represents an overall transgression from a vertically stacked fluvial channel bar in the base to a floodplain deposit at the top. Interbedded intervals with a coarsening-up texture and irregular sandstone beds are interpreted to be over-bank deposits spilling from the main channels.

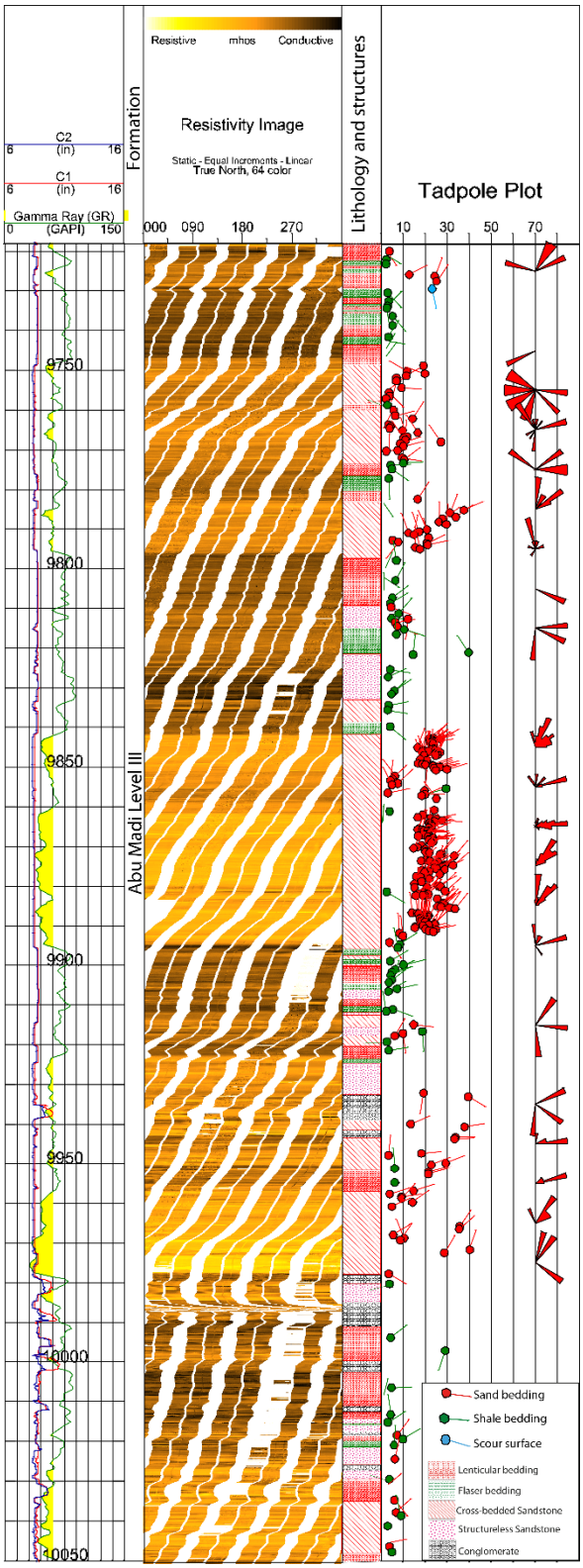

Fig. 8. FMI of the Level III sequence (South Batra-14 well).

4. Discussion

4.1 Comparison of the wells

From the image logs as well as seismic and composite logs, it is apparent that there have been several

episodes of regressions and transgressions during the Messinian time period, at least two different aged channel belts can be identified from the seismic (**Fig.9**). The youngest channel belt is the only one that has been penetrated by the wells in this area, and one can identify several episodes of transgression and regression within it as fining upward sequences on the GR log (**Fig.10**). All the wells that have been part of this study show this fining upward character in the Abu Madi Level III.

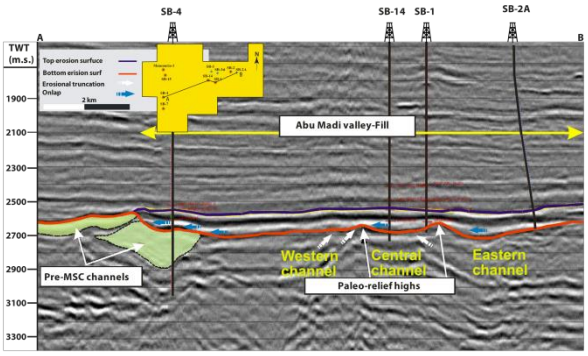

Fig. 9. Seismic line running across the incised valley from South Batra 4, via South Batra 14 and 1 out to South Batra 2a. The line shows several generations of channels, all located on the western side of the valley (El Adl, et al. 2021).

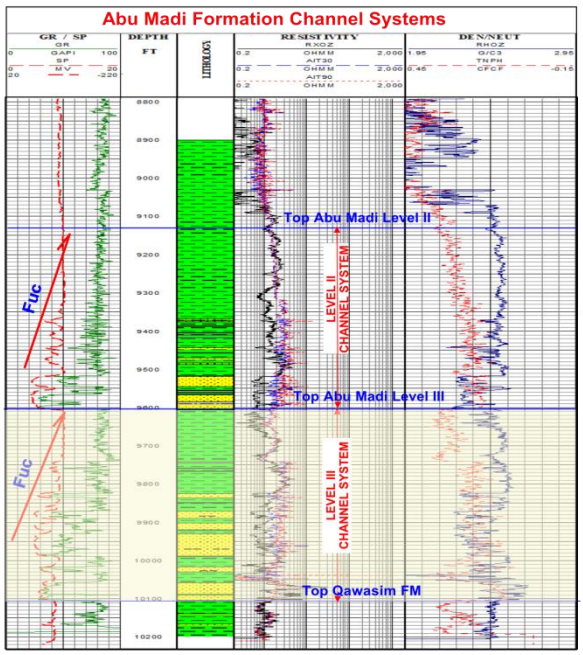

Fig. 10. Abu Madi Formation channels system showing transgressive cycle in Level III.

One of the objectives of this study was to investigate whether the sands that were considered Abu Madi Level III were deposited during the same regressive pulse. In a mixed fluvial and restricted marine or floodplain systems like the current one, correlating sands can often be misleading. To resolve this issue, the study focused on the shales overlying the sand package. It is very relevant to correlate this shale from well to well across the South Batra area using the image logs, which appears to support the assumption that the sands were deposited during the same cycle.

4.2 Facies Maps

A definite sedimentary facies is defined as a unit of rock that, owing to deposition in a particular environment, has a characteristic set of properties. Based on the information from the core, open hole, and image logs, two different facies are recognized in this system: a) Fluvial facies, which is characterized by a well sorted, clean sand with medium to high angle crossbeds and a uniform orientation; b) Floodplain facies where the lenticular and flaser bedding is observed and dominant of ripple marks and mudstone beds (**Fig.11**).

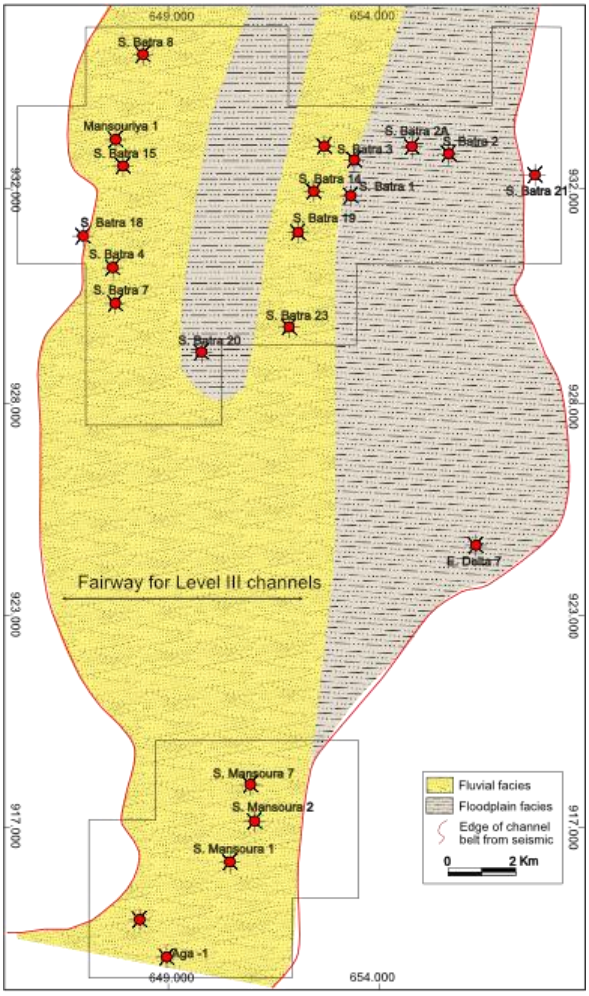

Fig. 11. Facies map over basal fluvial dominated part of Abu Madi Level III. Floodplain facies within the fluvial fairway is based on seismic.

The basal part of the Level III sand package changes laterally from fluvial at the western part of the field to floodplain deposits to the east. The interpretation of these sediments representing floodplain deposits within the fluvial fairway is based on the seismic amplitude map only due to a lack of well control.

On the image logs, it is hard to distinguish between floodplains and restricted marine facies in this micro-tidal setting. Our interpretation is based on what is known about the whole area and what makes the most sense geologically. In this case, with a structural dip of 1 – 2°, it would be hard to have fluvial channels on one side of the paleo-valley and restricted marine on the other just a few miles away. Floodplain deposits are a more likely type of deposition for the lower sands on the eastern side of the paleo-valley.

4.3 Isopach Maps

Separate isopach maps of the gross sand in Level III and for the fluvial sections were made using GR logs and image logs (**Fig.12**). The gross sand isopach shows the sands widespread over the whole area. Considering the locations of the wells; there is poor control in the area between the South Batra 4 and South Batra 14 wells, a distance of 6.2 miles. The isopach map of the fluvial section indicates that the focus of the channels is on the western side of the paleo-valley. The empty area between South Batra 4 and South Batra 14 is based on the amplitude map shown in **Figure 5**.

It is interesting to compare the isopach maps with a seismic line across the area, oriented E-W from South Batra 4 via South Batra 14 to South Batra 2 wells (**Fig.9**). It shows the incised paleo-valley very well. In addition, there are two older channels located on the western side of the valley in the same general area where the thickest package of Level III fluvial sands is located. This suggests that a deeper tectonic control has created a slight depression where the fluvial system is thickest. Also, note the high area west of South Batra 14 well. This feature, if present at the time of deposition, could have created a split in the river system resulting in two separated sands.

4.4 Flow Directions

Based on the recognition of current direction indicators from image logs, a flow direction map has been constructed (**Fig.13**). It can be seen that two orientations are dominant, NW and NE. Both orientations show a very narrow range of directional variation, which suggests a low sinuosity system such

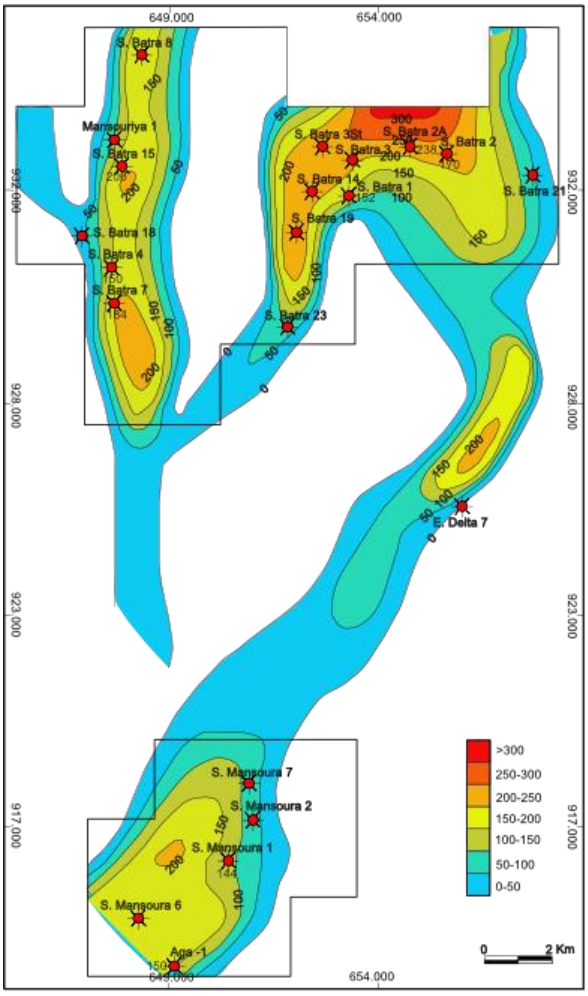

Fig. 12. Isopach map of the gross sand of the Abu Madi Level III.

as a braided river, as the method of deposition. Seismic indicates that the width of the incised paleo-valley is approximately 10 miles wide in the area. Within this paleo-valley, numerous smaller channels can be recognized on the images flowing mainly to the NE or the NW. The width of these channels is estimated based on the thickness of the bed forms identified on the image logs and ranges from 50 to 450 feet, with an average channel width of approximately 150 feet.

4.5 Depositional Model

The Abu Madi Formation is interpreted as a sequence of river/delta deposits which deposited immediately above the Qawasim unconformity (Alfy, et al. 1992).The salinity crisis took place between 5.96 and 5.33 million years ago when the marine passages between the Atlantic and the Mediterranean closed (Duggen et al. 2003). This caused the water to

evaporate and dropby ca 2000m, causing the Eonile fluvial channels to cut down into the underlying, mostly Tortonian, fluvio-deltaic sediments.

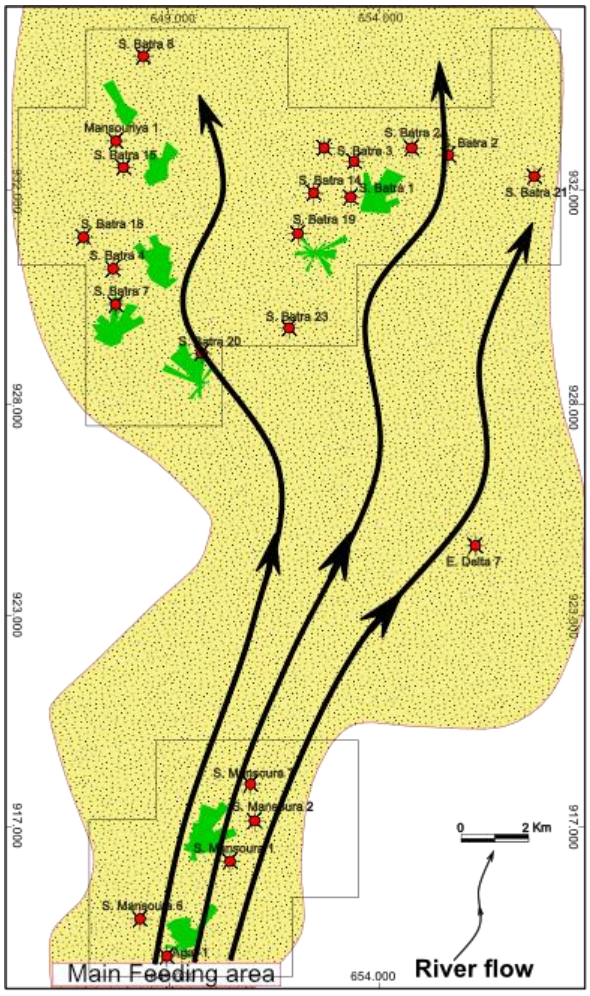

Fig. 13. Flow direction for the Abu Madi Level III showing a dominant flow towards NW and NE.

Investigation of the sedimentology, especially the ratio of sandstone to finer siltstones, suggested division of the Abu Madi Formation into three major sand levels. These, from the oldest to the youngest, were designated Level III, Level II and Level I. The main pay zones are located in Levels II and III (**Fig. 2**). Level III sands were deposited by braided-fluvial distributary channels, possibly in the lower delta plain. Based on sedimentological characteristics, FMI images and logs, the sequence of Level III is subdivided into two parts, lower and upper (**Fig. 14**). The lower and middle Level III sands are well-connected laterally, have a high sand-shale ratio and a sand-sheet geometry typical of a channel fill. This type of deposit has produced good quality reservoirs. In contrast, the upper-Level III unit is highly variable with rapid lateral changes in rock type and is thought to represent an estuarine environment, over-bank deposits and/or channel abandonment phase.

4.6 Petroleum System

The reservoir in the Abu Madi Level III sequence can be divided into two units: Fluvial sandstone reservoir and floodplain sandstone reservoir (**Fig.15**). The fluvial reservoir is created during the onset of a regressive period. Sand-dominated braided rivers occupied an incised paleo-valley and deposited sand bars. The sand in this part of the section is very clean and well-sorted (**Fig.15**).

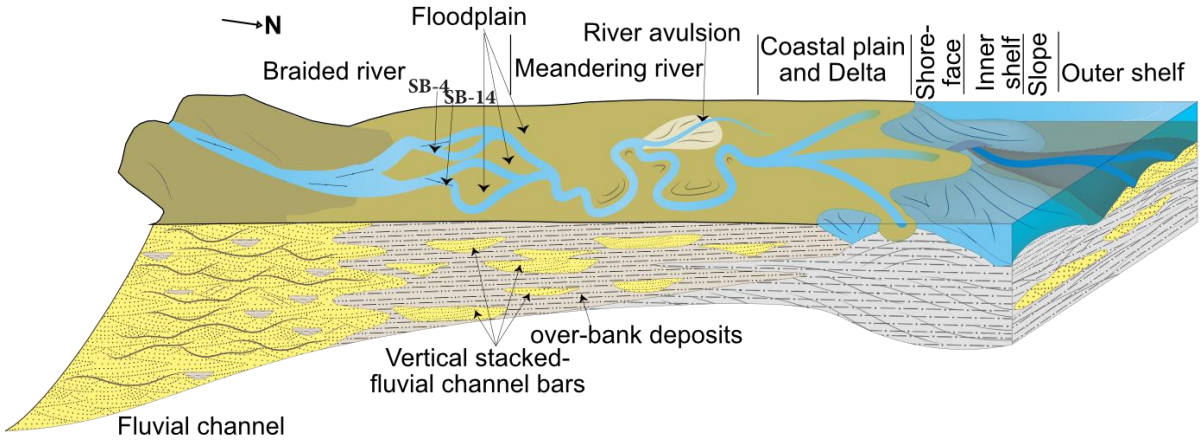

Fig. 14. A representative depositional model for the Abu Madi Level III.

The general shape of these deposits is likely elongated in the direction of the paleo-flow. Based on the vertical thickness of individual flow units identified on image logs in the fluvial section, the average sand bar is about 3' thick and up to 150' wide. A few beds measure up to 9 feet in thickness, which suggests a possible 450' wide channel. Typically, these bars occur stacked in multiple sequences (**Fig.15**). From the resistivity and caliper logs, it is obvious that this rock has good permeability. The porosity logs show good crossovers in the gas-bearing zones and indicate porosity of 15 – 25% in the reservoir intervals (**Fig.15**).With rising sea level, the incised valley gradually became flooded and floodplain conditions took over. The sand content in this section is still high, however, there is an increase in shale content. The shapes of these deposits are sheet-like. The thickest sand bodies are interpreted to be located in the area where the fluvial channels were active due to the reworking of previously deposited sands. Permeability and porosity values are comparable to the fluvial section.

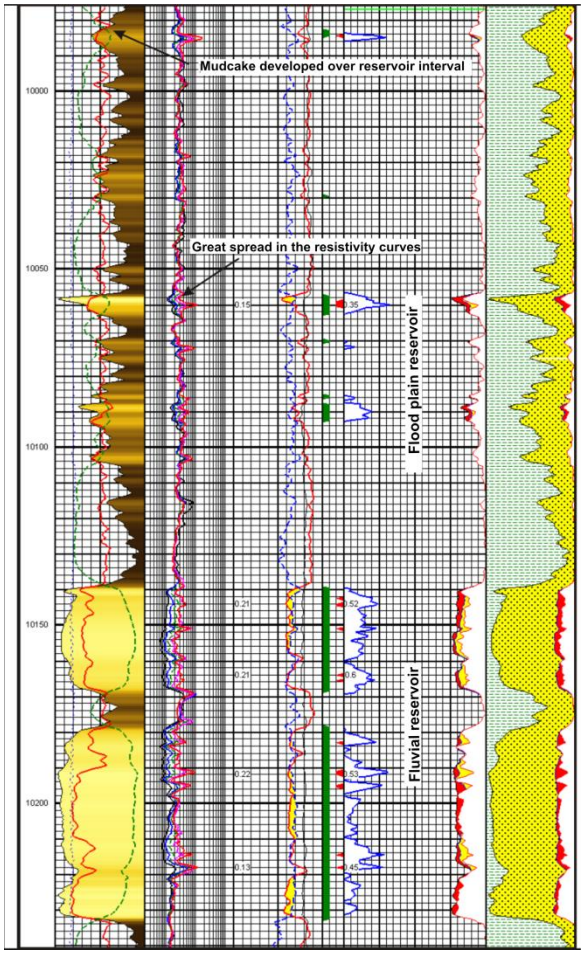

Fig. 15. Formation evaluation example showing the mudcake development, resistivity spread, and porosity crossovers in South Batra wells.

However, it is beyond the scope of this study to determine the source rock for the Abu Madi in the area, it appears that the source has gone through the oil window and is in or has also passed the gas window. Leila and Moscariello, 2017 concluded that the Miocene gas in the El Mansoura Concession originated from a Jurassic source rock due to the wet gas window maturity. The condensates purged from the source rock were the first hydrocarbons to be trapped in the El Mansoura Field. During this initial phase, the hydrocarbons appear to have been trapped stratigraphically in discreet sands in the fluvial system. These traps were created where the sand-rich braided river system pinched out into shaly floodplain deposits (**Figs. 5 and 11**). It appears that this formed the only trapping mechanism at this time.

Overlying the fluvial sands containing the condensate is a tighter zone, which appears to have seal capacities to hold the condensate but is permeable to the gas. In the core from South Batra 14, there is also 6 feet-thick mudstone, which may act as a vertical seal (Figs. 3g and 4). This interpretation is consistent with the amplitude map around the South Batra 14 well (**Fig.5**). It indicates an isolated pod of sand (yellow colors) around this well. To the west and up-dip, the sand shales out as supported by the darker colors on the map.

The subsequent expulsion of gas from the source rock filled whatever could be trapped in the reservoir, either in the fluvial or the floodplain reservoir sands. It is suggested that the main trapping mechanism at this time was of a structural nature. Support for this interpretation is seen on a 2D seismic line, which runs through the South Batra area and through the town of Mansoura (**Fig.16**). Calculations from the 2D line and the 3D seismic data east of this puts the fault throws in the range from 75' to 200'. As can be seen in Figure 22, the faults are downthrown to the north.

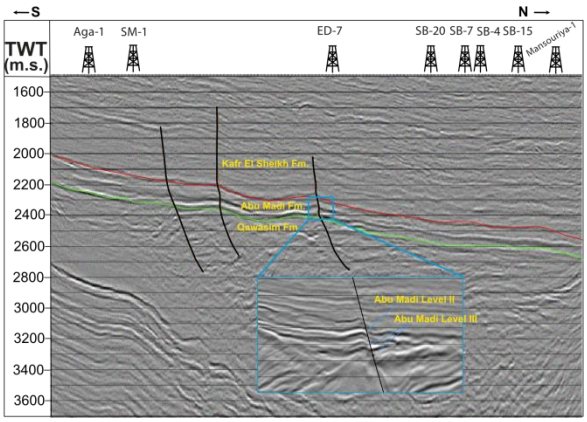

Fig. 16. A 2D line showing faulting indicated with black lines. There are more faults than is indicated; only the largest ones are marked.

This regional fault system strikes E – W all the way to the East Delta 7 well and turns NE – SW around that well. To seal off the entire sand package in the South Batra 7 well, a fault with a minimum throw of 195' is needed. Based on the observations from the seismic, the faults are capable to do this. The faults are located to the north of South Mansoura 1 and Aga 1 boreholes and are possibly the reason why these wells are wet. In the area south of South Batra 4 and 7 wells, there is a theoretical possibility that the channels shale out and stratigraphically trap the hydrocarbons. However, given what we know about the amounts of sand in this system, the chance of this is considered very small. Wells in the field are charged with gas at depths below the depth of the condensate in South Batra 14, which indicates that this whole system has not reached equilibrium yet.

5. Conclusions

- The Abu Madi Level III sequence is interpreted to have been deposited as valley fill sediments within a pre-existing paleo-valley during a regressive-transgressive sedimentary cycle. The valley was most likely created during the Messinian salinity crisis, which happened as a result of the closure of the marine passages between the Atlantic and the Mediterranean oceans about 5.96 – 5.33 m.y.
- From the image logs, the river systems feeding sand into the Mediterranean was a sand dominated braided river system. The channels making up the braided system were on average 150 feet wide. Following the regression, the valley was flooded, and floodplain conditions took over.
- Reservoirs in the fluvial section are very clean and well sorted. Their shape is elongated parallel to the paleo-flow and most likely interconnected over the entire width of the fluvial tract.
- Reservoirs in the floodplain section have a higher shale content compared to the fluvial system. The shape of these reservoirs is most likely restricted sheet like parallel to the valley system confining boundaries.
- Condensate is stratigraphically trapped in the fluvial section, which is pinching out into floodplain deposits.
- Gas is mainly structurally trapped in floodplain and fluvial reservoirs.
- Based on this study, our recommendation is to do additional drilling to the south of South Batra 7. This is because the reservoir in this area is mainly fluvial sand bodies, which create a cleaner and better-sorted reservoir compared to the floodplain sands, and because the fluvial section is thickest in this area.

Ethics approval and consent to participate: This article fulfills the known research ethics related to geological studies. .

Consent for publication: The author declares his consent for publication.

Funding: There is no funding taken for this paper.

Conflicts of Interest: The author declares no conflict of interest.

Contribution of Authors: This work is a single-author contribution and all work steps were carried out by the author himself, except as noted.

Acknowledgments: The author would like to express his deep graduate to the Egyptian General Petroleum Corporation (EGPC) and Mansoura Petroleum Company for providing the data and the permission to publish this study.

6. References

Alfy, M., Polo, F.,Shash, M.(1992) The geology of Abu Madi gas field. Proceedings of the 11th Petroleum Exploration and Production Conference, Cairo, 485-513.

Bache, F., Olivet, J.L., Gorini, C., Rabineau, M., Baztan, J., Aslanian, D., Suc, J.P. (2009) Messinian erosional and salinity crises: view from the provence basin (Gulf of Lions, Western Mediterranean). Earth and Planetary Science Letters, 286, 139-157.

Barber, P. (1981) Messinian subaerial erosion of the proto-Nile Delta. Marine Geology, 44, 253-272.

Cant, D.J. (1978) Development of a facies model for sandy braided river sedimentation: Comparison of the South Saskatchewan River and Battery Point Formation. In: Miall, A.D. (ed.) Fluvial Sedimentology, C.S.P.G Memoir, 5, 627 – 640.

Claudio, F., Glišović, P., Alessandro, F., Becker, T.W., Garzanti, E., Sembroni, E., Gvirtzman, Z. (2019) Role of dynamic topography in sustaining the Nile River over 30 million years. Nature Geoscience, 12, 1012-1017.

Clauzon, G. (1982) Le canyon Messinien du Rhône: unepreuvedécisive du 'dessicated deep-basin model' (Hsü, Cita and Ryan, 1973). Bulletin de la SocieteGéologique de France 24, 231-246.

Donselaar, M.E., Schmidt, J.M. (2005) Integration of outcrop and borehole image logs forhigh-resolution facies interpretation: example from a fluvial fan in the Ebro Basin, Spain. Sedimentology, 52 (5), 1021–1042.

Duggen, S., Hoernie, K., van den Bogaard, P., Rupke, L., Phipps, M.J. (2003) Deep roots of the Messinian salinity crisis: Nature, 422, 602 – 605.

El-Adl, H., Leila, M., Ahmed, A., Anan, T., El-Shahat, A. (2021) Integrated sedimentological and petrophysical rock-typing of the messinian Abu Madi formation in

south Batra gas field, onshore Nile Delta, Egypt. Mar. Petrol. Geol., 124, 104835.

Fielding, L., Najman, Y., Millar, I., Butterworth, P., Garzanti, E., Vezzoli, G., Barfod, D., Keneller, B. (2018) The initiation and evolution of the River Nile. Earth Planetary Science Letters, 489, 166-178.

Folkestad, A., Veselovsky, Z., Roberts, P. (2012) Utilising borehole image logs to interpret delta to estuarine system: a case study of the subsurface Lower Jurassic Cook Formation in the Norwegian northern North Sea. Mar. Petrol. Geol., 29 (1), 255–275.

Galloway, W.E., Hobday, D.K. (1983) Terrigenous clastic depositional systems. Springer–Verlag, New York, Berlin, Heidelberg, Tokyo, 423 p.

Hassan, S., Darwish, M., Tahoun, S.S., Radwan, A.E. (2022) An integrated high-resolution image log, sequence stratigraphy and palynofacies analysis to reconstruct the Albian–Cenomanian basin depositional setting and cyclicity: insights from the southern Tethys. Mar. Petrol. Geol., 137, 105502.

Hsü, K.J., Cita, M.B., Ryan, W.B.F. (1973) The origin of the Mediterranean evaporites, in A. Kaneps Ed, Leg 13, Initial Reports of the Deep Sea Drilling Project, 13 (2), 1203-1231.

Issawi, B., McCauley, J.F. (1992) The Cenozoic rivers of Egypt: the Nile problem. In: Adams, B., Friedman, R., (eds.), The Followers of Horus: studies dedicated to Michael Allen Hoffman 1944-1990: Egyptian Studies Association Publication, 2, Oxbow Press, Oxford, United Kingdom, 121-138.

Lai, J., Wang, G., Wang, S., et al. (2018) A review on the applications of image logs in structural analysis and sedimentary characterization. Mar. Petrol. Geol., 95, 139–166.

Leeder, M. (1973) Sedimentology and paleogeography of the upper old red sandstone in the Scottish border basin. Scottish Journal of Geology, 9, 117-144.

Leila, M., Moscariello, A. (2017)Organic geochemistry of oil and natural gas in the West Dikirnis and El-Tamad fields, onshore Nile delta, Egypt: interpretation of potential sourcerocks. Journal ofPetroleum Geology, 40, 37- 58.

Leila, M, Moscariello, A. and Šegvić, B. (2018) Geochemical constraints on the provenance and depositional environment of the Messinian sediments, onshore Nile Delta, Egypt, Implications for the late Miocene paleogeography of the Mediterranean. Journal of African Earth Sciences, 143, 215-241.

Leila, M., Moscariello, A. (2019) Seismic stratigraphy and sedimentary facies analysis of the pre- and syn-Messinain salinity crisis sequences, onshore Nile Delta, Egypt, Implications for reservoir quality prediction. Marine and Petroleum Geology, 101, 303-321.

Lloyd, P.M., Dahan, C., Hutin, R. (1986) Formation imaging with microelectrical scanning arrays - a new generation of high resolution dipmeter tool. Trans 10th Europ Form Eval Symp Soc Prof Well Log Analysts: Paper L.

Merlose, (2007) Seismic Sequence Stratigraphic and Facies Architecture of Miocene Reservoirs in South Batra Field. 8, 84 – 87 (Unpublished Internal Report).

Metwalli, M.H. (2000) A new concept for the petroleum geology of the Nile Delta, A. R. Egypt. International Conference Geology of the Arab World (GAW), Cairo Univ., Cairo 2, 713-734.

Miall, A.D. (1977) A review of the braided river depositional environment. Earth Science Review, 13, 1-62.

Miall, A.D. (2014) Fluvial Depositional Systems, vol. 14. Springer International Publishing, Cham, p. 316.

Nabawy, S., Basal, A., Sarhan, M., Safa, M. (2018) Reservoir zonation, rock typing and compartmentalization of the Tortonian-Serravallian sequence, Temsah Gas Field, offshore Nile Delta, Egypt. Marine and Petroleum Geology, 92, 609-631.

Orton, G., Reading, H. (1993) Variability of deltaic processes in terms of sediment supply, with particular emphasis on grain size. Sedimentology, 40, 475–512.

Reineck, H., Singh, I. (1980) Depositional Sedimentary Environments; with Reference to Terrigenous Clastics. Springer, Heidelberg, 549p.

Said, R. (1990) The Geology of Egypt. A. Balkema Publishers, USA, 734 p.

Schlumberger, (1995) Well Evaluation Conference Egypt, 57-71.

Serra, O. (1989) Formation MicroScanner Image Interpretation. Schlumberger Educational Services Publication, Houston, PubL No. SMP-7028.

Sestini, G. (1995) Egypt, in H. Kulke Ed, Regional Petroleum Geologyof The World, Part II, Africa, America, Australia and Antarctica (Beiträge zur regionalen Geologie der Erde 22, 66-87, Gebrüder Borntraeger Verlagsbuchhandlung, Stuttgart.

Tucker, M. (2001) Sedimentary Petrology. Blackwell Scientific, Oxford, p. 272.

Willett, S., Schlunegger, F., Picotti, V. (2006) Messinian climate change and erosional destruction of the central European Alps. Geology, 34(8), 613-616.

البيئة الترسيبية وآلية احتجاز الغاز والمكثفات في المستوى الثالث لمتكون أبو ماضي المسيني، دلتا النيل، مصر

أحمد جمعه محمد
قسم الجيولوجيا، كلية العلوم، جامعة المنصورة، مصر

يُفسر تتابع المسيني من المستوى الثالث لمتكون أبو ماضي على أنه قد تم ترسيبه على شكل رواسب نهرية خلال دورة رسوبية تراجعية متعدية. تم إنشاء الوادي على الأرجح خلال أزمة الملوحة الميسينية، والتي حدثت بسبب إغلاق الممرات البحرية بين المحيط الأطلسي والبحر الأبيض المتوسط. تم استخدام الصور اللبية والتصوير المصغر للمتكونوسجلات الآبار المختلفة لتحديد بيئة الترسيب ونظام البترول في منطقة الدراسة. من الصور اللبية وسجلات الصور، كان نظام النهر الذي يغذي الرمال في البحر الأبيض المتوسط عبارة عن نهر مضفر تسوده الرمال. كان متوسط عرض القنوات المكونة للنظام المضفر ١٥٠ قدمًا. وفي أعقاب هذا التراجع، غمرت المياه الوادي، واستولت على الودائع المصرفية. الخزانات في القسم النهري جيده جدا وخالية من الطين. شكلها ممدود ومتوازي مع التدفق القديم ومن المرجح أن يكون مترابطًا على كامل عرض القناة النهرية.تحتوي الخزانات الموجودة في القسم العلوي من الضفة على محتوى طيني أعلى مقارنة بالنظام النهري. من المرجح أن يكون شكل هذه الخزانات مقيدًا مثل الصفائح بالتوازي مع نظام الوادي الذي يحصر الحدود. يتم احتجاز المكثفات بشكل طبقي في القسم النهري، الذي يتدفق إلى رواسب السهول الفيضية. يتم حجز الغاز بشكل أساسي من الناحية الهيكلية في السهول الفيضية والخزانات النهرية.